PNAS
www.pnas.org

Supplementary Information for

Fibroblast growth factor receptor influences primary cilium length through an interaction with intestinal cell kinase

Michaela Kunova Bosakova, Alexandru Nita, Tomas Gregor, Miroslav Varecha, Iva Gudernova, Bohumil Fafilek, Tomas Barta, Neha Basheer, Sara P. Abraham, Lukas Balek, Marketa Tomanova, Jana Fialova Kucerova, Juraj Bosak, David Potesil, Jennifer Zieba, Jieun Song, Peter Konik, Sohyun Park, Ivan Duran, Zbynek Zdrahal, David Smajs, Gert Jansen, Zheng Fu, Hyuk Wan Ko, Ales Hampl, Lukas Trantirek, Deborah Krakow*, Pavel Krejci*

Pavel Krejci
Email: krejcip@med.muni.cz

Deborah Krakow
Email: dkrakow@mednet.ucla.edu

This PDF file includes:

Figs. S1 to S5

A

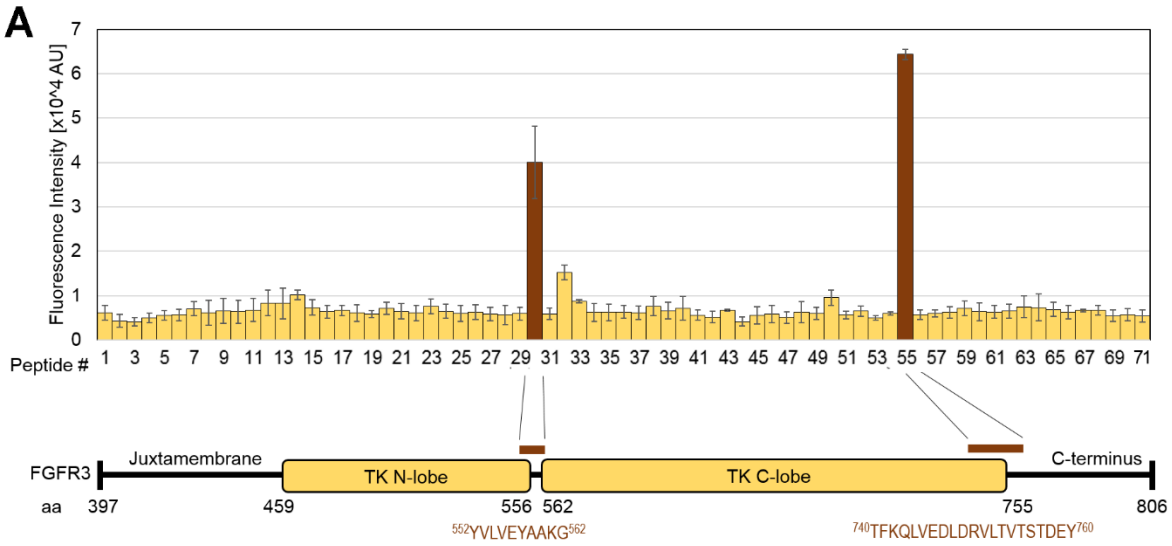

B

Peptide #	Peptide sequence	Fluorescence	Peptide #	Peptide sequence	Fluorescence
1	397RLRSPPKKGLGSP409	6182	37	590TFKDLVSCAYQVARGMEYLASQ611	6138
2	400SPPKKGLGSPTVH412	4314	38	590TFKDLVSCAYQVARGMEYLA609	7629
3	403KKGLGSPTVHKIS415	4106	39	612KCIHRDLAARNVLVT626	6606
4	406LGSPTVHKISRFP418	4982	40	627TEDNVMKIADFGL638	7081
5	409PTVHKISRFPLKR421	5550	41	630NVMKIADFGLARD641	5617
6	412HKISRFPLKRQVS424	5647	42	633KIADFGLARDVHN644	5181
7	415SRFPLKRQVSLES427	7046	43	636DFGLARDVHNLDY647	6670
8	418PLKRQVSLESNAS430	6104	44	639LARDVHNLDYYKK650	4154
9	421RQVSLESNASMSS433	6550	45	642DVHNLDYYKKTTN653	5494
10	424SLESNASMSSNTP436	6372	46	645NLDYYKKTTNGRL656	5860
11	427SNASMSSNTPLVR439	6770	47	648YYKKTTNGRLPVK659	5111
12	430SMSSNTPLVRIAR442	8335	48	657PVKWMAPEALFDRVY671	6331
13	433SNTPLVRIARLSS445	8241	49	689TLGGSPYPGI698	5915
14	436PLVRIARLSSGEG448	10174	50	699PVEELFKLLKE709	9525
15	439RIARLSSGEGPTL451	7331	51	710GHRMDKPANC719	5642
16	442RLSSGEGPTLANV454	6352	52	720THDLYMIMRECW731	6490
17	445SGEGPTLANVSEL457	6694	53	732HAAPSQRP739	4963
18	448GPTLANVSELELP460	6084	54	740TFKQLVEDLDRVLTV754	5997
19	451LANVSELELPADP463	5899	55	740TFKQLVEDLDRVLTVTSTDEY760	64339
20	454VSELELPADPKWE466	7129	56	748LDRVLTVTSTDEY760	5661
21	457LELPADPKWELSR469	6475	57	751VLTVTSTDEYLDL763	5965
22	459LPADPKWEL467	6094	58	754VTSTDEYLDLSAP766	6255
23	468SRARLTLGKPLGE480	7629	59	757TDEYLDLSAPFEQ769	7135
24	481GCFGQVVMAEA491	6483	60	760YLDLSAPFEQYSP772	6385
25	492IGIDKDRAAKP502	6001	61	763LSAPFEQYSPGGQ775	6325
26	503VTVAVKMLKDDA514	6240	62	766PFEQYSPGGQDTP778	6493
27	515TDKDLSDLVSEMEMMKMIG533	5891	63	769QYSPGGQDTPSSS781	7493
28	533GKHKNIIN540	5644	64	772PGGQDTPSSSSSG784	7337
29	541LLGACTQGGPL551	5977	65	775QDTPSSSSSGDDS787	6882
30	552YVLVEYAAKG561	40066	66	778PSSSSSGDDSVFA790	6318
31	556EYAAKGNLREFLRA569	5912	67	781SSSGDDSVFAHDL793	6640
32	565EFLRARRPPGLDY577	15259	68	784GDDSVFAHDLLPP796	6689
33	568RARRPPGLDYSFD580	8758	69	787SVFAHDLLPPAPP799	5476
34	571RPPGLDYSFDTCK583	6236	70	790AHDLLPPAPPSSG802	5740
35	574GLDYSFDTCKPPE586	6215	71	793LLPPAPPSSGGSRT806	5400
36	577YSFDTCKPPEEQL589	6335			

Figure S1 Mapping the FGFR3-ICK interaction using peptide microarray
(A) The intracellular part of FGFR3 was dissected into 71 overlapping peptides, and the peptide microarray was prepared and processed as detailed in Material and Methods. The fluorescence signal corresponds to ICK binding, and identified two ICK-binding peptides: 552YVLVEYAAKG561, and 740TFKQLVEDLDRVLTVTSTDEY760. TK, tyrosine kinase. (B) Table listing all peptides and the corresponding mean of fluorescence values. The ICK interacting peptides are highlighted

in red. The contribution of ^{740}TFKQLVEDLDRVLTVTSTDEY^{760} to FGFR3-ICK interaction is further analyzed in the manuscript (Figs. 2, 3). The identification of additional ICK binding site (^{552}YVLVEYAAKG^{562}) in the kinase domain of FGFR3 is in discrepancy with the co-immunoprecipitation results, where all C-terminal truncated constructs failed to bind ICK, despite possessing the intact ^{552}YVLVEYAAKG^{562} motif (Fig. 2B). It is likely that the ^{552}YVLVEYAAKG^{562} motif is a weak binding site that is not sufficient alone to mediate the stable interaction between FGFR and ICK, necessary for co-immunoprecipitation.

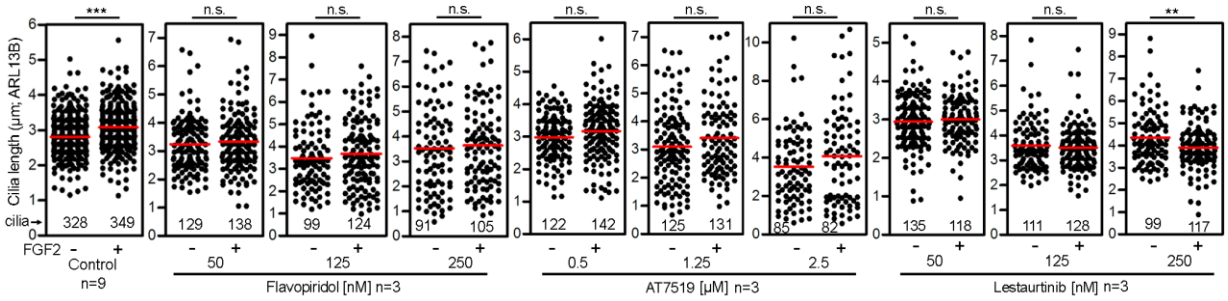

Figure S2 Inhibition of Ick activity deregulates cilia length and blocks the FGF2-mediated cilia elongation.
NIH3T3 cells were serum starved for 12 hours to produce cilia, and then treated with ICK inhibitors flavopiridol, AT7519 or lestaurtinib, in the presence or absence of 2 ng/ml FGF2 for additional 12 hours. Cilia were visualized by ARL13B immunostaining, measured in 3D and plotted. Black dots, individual cilia; red bars, medians (Student´s t-test, ***$p<0.001$); n.s., not significant.

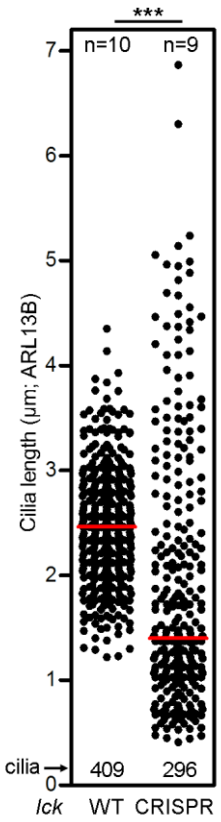

Figure S3 *Ick*^{CRISPR} NIH3T3 cells form cilia with extreme variability in length
NIH3T3 cells were serum starved (24-36 hours) before their cilia lengths were visualized by ARL13B immunostaining, measured and plotted. Black dots represent individual cilia; red bars show medians (Student´s t-test, ***$p<0.001$). Cilia of non-transfected FGF2-naïve wild-type (WT) and *Ick*^{CRISPR} NIH3T3 cells from Figure 6 and Figure 7F were used to build the figure.

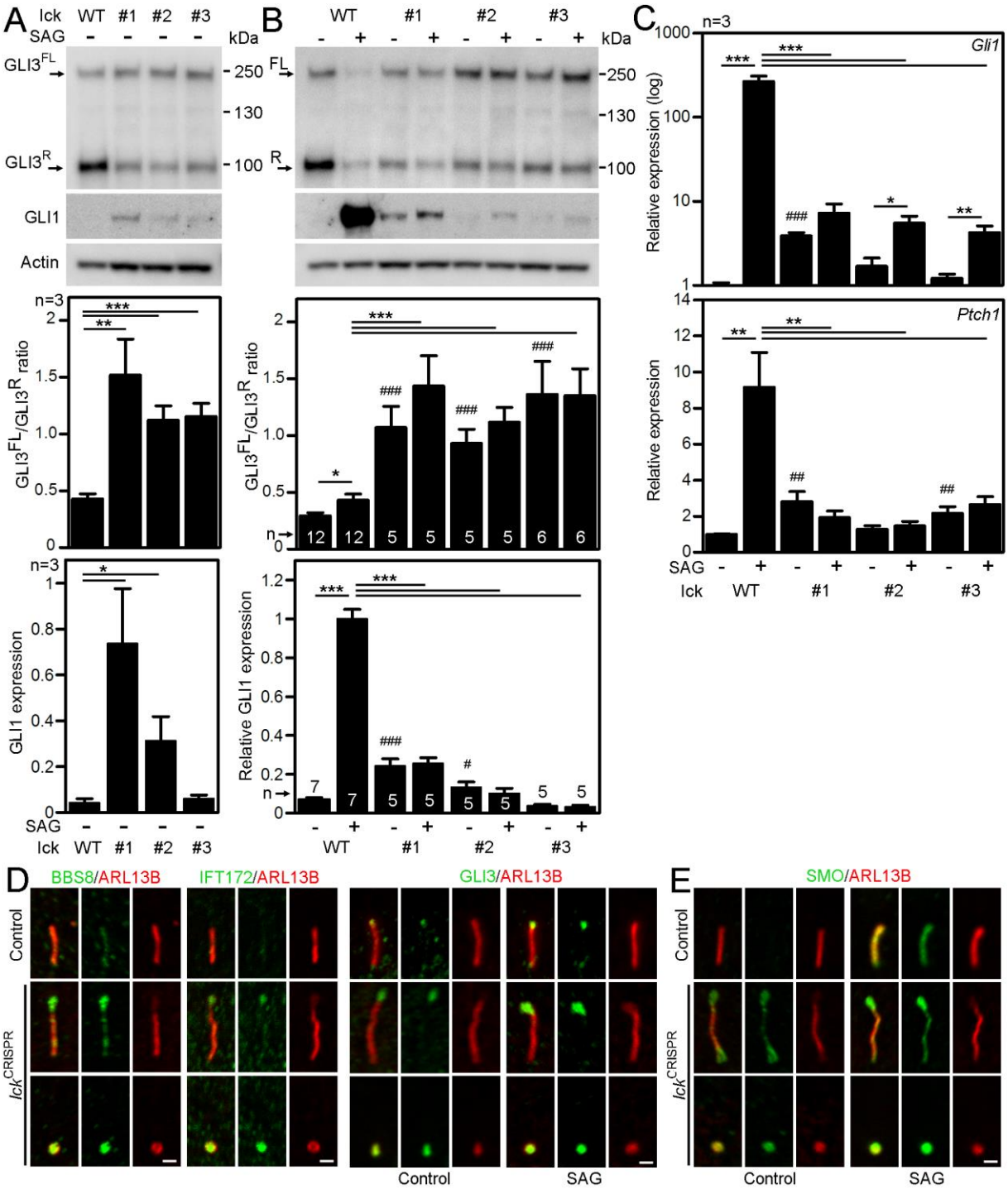

Figure S4 *Ick*^{CRISPR} NIH3T3 cells have deregulated IFT and Hedgehog signaling

(A) GLI3 expression in *Ick*^{CRISPR} cells (clones #1, #2, and #3), analyzed by western blot. *Ick*^{CRISPR} cells show increased full length GLI3 (FL) to repressor (R) ratio, and upregulate GLI1, compared to wild-type (WT) NIH3T3 cells (Student´s t-test, $^{*/\#}p<0.05$, $^{**/\#\#}p<0.01$, $^{***/\#\#\#}p<0.001$). Actin was used as a loading control and for normalization of GLI1 expression. (B-C) *Ick*^{CRISPR} cells do not process GLI3 upon treatment with SAG, as evidenced by no changes in GLI3^{FL}/GLI3^{R} ratios, fail to activate GLI1 expression in western blots (B), and *Gli1* and *Ptch1* expression in qRT-PCR (C) (statistical significance - # among untreated cells, * among SAG treated cells). (D) Cilia of *Ick*^{CRISPR} cells aberrantly accumulate BBS8, IFT172 and GLI3 in their bulged tips. (E) In the absence of SAG, *Ick*^{CRISPR} cells translocate Smoothened (SMO) to cilia in contrast to

WT cells that do so only in response to SAG treatment.

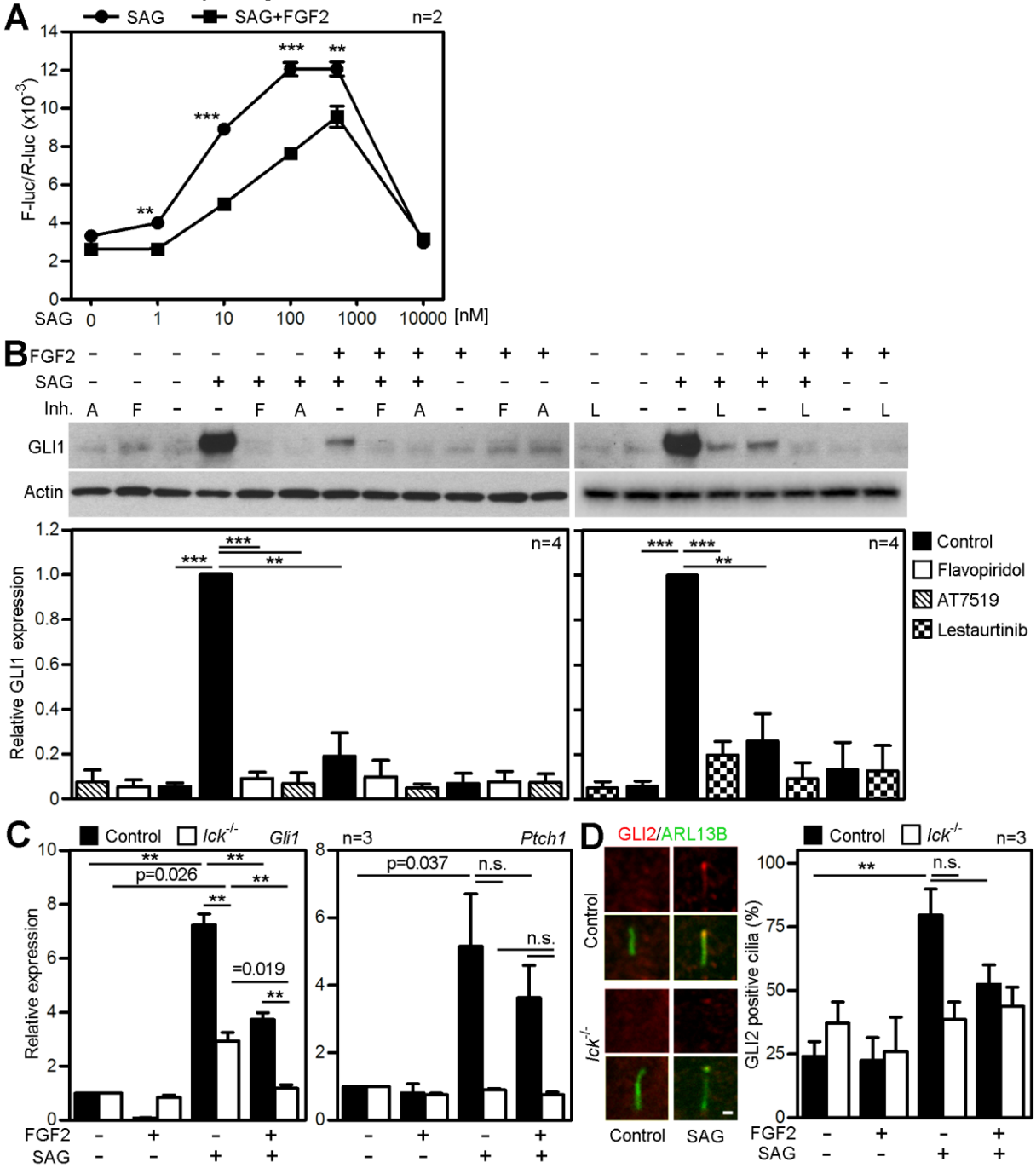

Figure S5 Downregulation of Ick activity inhibits Hh signaling

(A) Serum starved Shh-LIGHT2 NIH3T3 cells were treated with increasing concentrations of SAG. FGF2 inhibited the SAG-mediated transactivation of the Hh reporter (Student´s t-test, **p<0.01, ***p<0.001). (B) Inhibition of ICK activity by 125 nM flavopiridol (F), 1.25 µM AT7519 (A), 125 nM lestaurtinib (L) or by FGF2 blocks the SAG-mediated GLI1 expression in NIH3T3 cells. Actin was used as a loading control, and for normalization of GLI1 expression. (C) Micromasses produced from limb buds of *Ick*$^{-/-}$ E12 mice have inhibited SAG-mediated expression of *Gli1* and *Ptch1*, compared to the *Ick*$^{+/+}$ littermates (control) that inhibit SAG-mediated *Gli1* expression upon FGF2. (D) *Ick*$^{-/-}$micromasses failed to efficiently shuttle GLI2 to cilia as a response to SAG, similar to FGF2-treated control micromasses. Cells were stained by ARL13B and GLI2 antibodies, and the percentage of GLI2-positive cilia was scored (scale bar 1 µm).